Level structure of ^{120}Sn: High resolution (p,t) reaction and shell model description

P. Guazzoni,[1] M. Jaskola,[1,*] L. Zetta,[1] A. Covello,[2] A. Gargano,[2] Y. Eisermann,[3] G. Graw,[3] R. Hertenberger,[3] A. Metz,[3] F. Nuoffer,[4] and G. Staudt[4]

[1]*Dipartimento di Fisica dell'Università and Istituto Nazionale di Fisica Nucleare, via Celoria 16, I-20133 Milano, Italy*

[2]*Dipartimento di Scienze Fisiche, Università di Napoli Federico II, and Istituto Nazionale di Fisica Nucleare, Complesso Universitario di Monte S. Angelo, Via Cintia-I-80126 Napoli, Italy*

[3]*Sektion Physik der Universität München, D-85748 Garching, Germany*

[4]*Physikalisches Institut, Universität Tübingen, Auf der Morgenstelle 14, D-72076 Tübingen, Germany*

(Received 29 March 1999; published 27 September 1999)

The (p,t) reaction on ^{122}Sn has been studied in a high resolution experiment at an incident proton energy of 26 MeV. The cross section angular distributions for transitions to 38 levels of ^{120}Sn with an excitation energy up to $\sim$3500 keV have been measured. Distorted wave Born approximation analysis of experimental angular distributions using double-folded potential for the exit channel has been done. This has made it possible to confirm previous spin and parity values and to propose new assignments for a large number of states. A shell-model study of ^{120}Sn has been performed using a realistic effective interaction derived from the Paris nucleon-nucleon potential. The calculations have been carried out within the framework of the seniority scheme including states with seniority up to 4. Comparison of the calculated and experimental spectra shows a one-to-one correspondence between levels up to about 2.7 MeV excitation energy and lends support to some of the spin-parity assignments given in this work. [S0556-2813(99)03210-0]

PACS number(s): 25.40.Hs, 21.10.Hw, 21.60.Cs, 27.60.+j

I. INTRODUCTION

The Sn isotopes have long been the subject of much experimental and theoretical work aimed at understanding their shell-model structure.

From the experimental point of view the level structure of the stable Sn isotopes, and in particular that of ^{120}Sn which is the subject of the present work, has been extensively studied by different kinds of nuclear reactions, especially those induced by light projectiles. In particular, the level scheme of ^{120}Sn has been investigated by means of inelastic scattering of protons [1], deuterons [2], ^{3}He and α [3,4], lithium ions [5,6], and by using the following one-, two-, and multinucleon transfer reactions ^{119}Sn(d,p) [7], ^{119}Sn(t,d) [8], ^{121}Sb$(d,{}^3\mathrm{He})$ [9], ^{121}Sb(t,α) [10], ^{122}Sn(p,t) [11], ^{118}Sn(t,p) [12], ^{123}Sb(p,α) [13], and ^{124}Te$(d,{}^6\mathrm{Li})$ [14]. More information has been obtained by the study of the decay of ^{120}In [15–18] and ^{120}Sb [15,19,20], as well as by γ-ray spectroscopy using the reactions (n,γ), $(n,n'\gamma)$, (γ,γ'), $(p,p'\gamma)$ [21–24] and Coulomb excitation [24,25]. The results obtained in these works are summarized in Refs. [26,27].

The (p,t) reaction on ^{122}Sn was first measured by Fleming *et al.* [11] at an incident energy of 20 MeV, with an energy resolution of 25 keV. However, in this experiment, which involved several even Sn isotopes, only the most intense transitions were measured. As a consequence, only eleven states in the residual nucleus were identified up to an excitation energy of $\sim$3 MeV.

On these grounds, it seemed to us interesting to perform a new study of the ^{122}Sn$(p,t)^{120}$Sn reaction. This was done in a high resolution experiment at 26 MeV incident energy. Accurate measurements of the differential cross sections allowed also to identify spin and parity of very weakly populated states in ^{120}Sn, with a lower limit for the integrated cross section of only a few μb. In all, we observed 38 states up to an excitation energy of $\sim$3.5 MeV.

Along with our experimental work, we have also performed a shell-model study of ^{120}Sn, in which we assume that ^{100}Sn is a closed core and let the valence neutrons occupy the five single-particle (sp) orbits $0g_{7/2}$, $1d_{5/2}$, $1d_{3/2}$, $2s_{1/2}$, and $0h_{11/2}$. Within this model space, however, the size of the energy matrices to be set up and diagonalized is very large. To circumvent this difficulty one has to resort to some truncation method. In single-closed-shell nuclei, such as the Sn isotopes, the seniority scheme provides a most appropriate tool to reduce the numerical work required by a complete-basis diagonalization. In our study of ^{120}Sn we have made use of a non-conventional approach to shell-model problems within the seniority scheme, which is based on a chain calculation across nuclei differing by two in nucleon number. A brief description of this approach, which we call chain-calculation method (CCM), is given in Sec. V A while a detailed account and some applications can be found in Refs. [28,29]. The main feature of this method is that, at each step of the chain calculation, we make use of a correlated basis. As we shall see in Sec. V A, this has the advantage to make it possible to further reduce seniority-truncated shell-model spaces without significant loss in the accuracy of the results. The use of correlated basis is a feature common to other approaches, among which we may mention here the multistep shell-model method [30].

In the present calculation we have included states with seniority up to 4. As regards the two-body interaction be-

*Permanent address: Soltan Institute for Nuclear Studies, Warsaw, Poland.

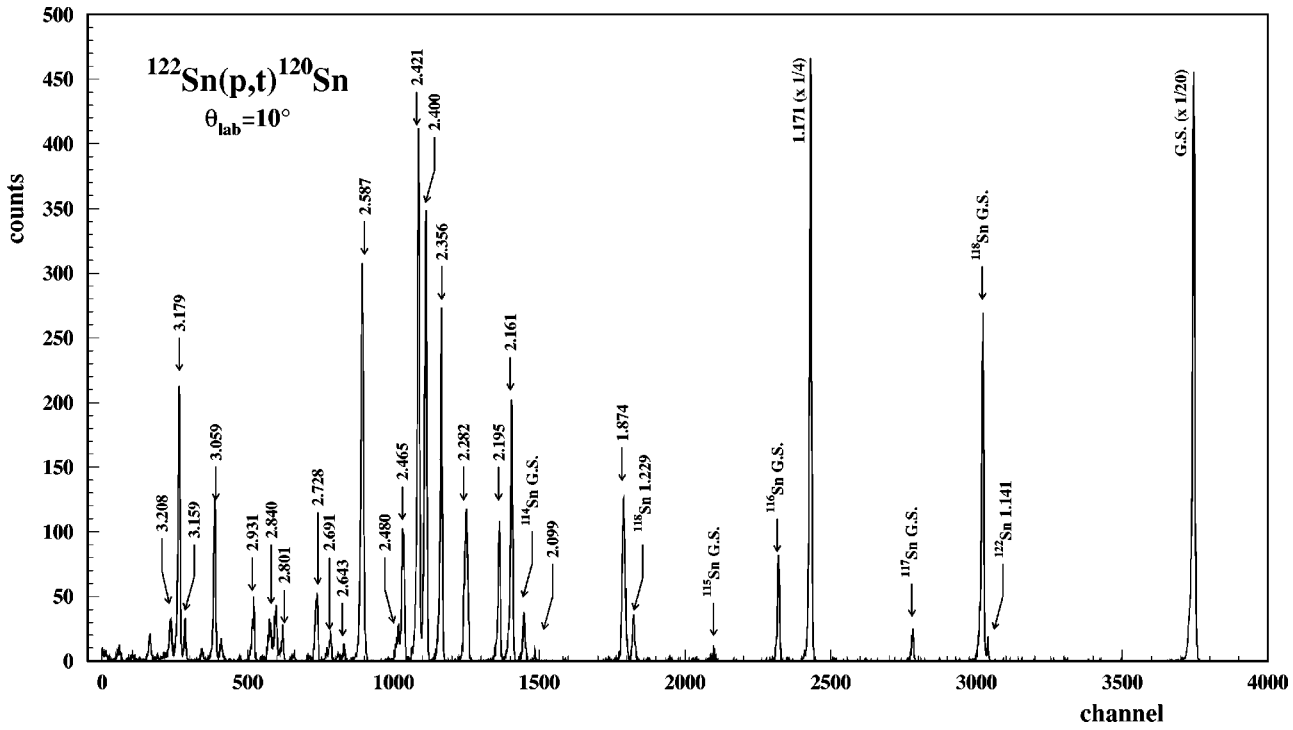

FIG. 1. The triton spectrum at 10° is shown and the excitation energies of the most prominent peaks are indicated. The position of the ground states of the different Sn isotopes are identified on the basis of *Q*-value differences [35].

tween the valence neutrons, we have employed a realistic effective interaction derived from the Paris free nucleon-nucleon potential [31] which has already produced quite satisfactory results for the heavier Sn isotopes [28,32].

The paper is organized as follows. In Sec. II the experimental apparatus is described. Section III compares the experimental results and DWBA calculations, using double-folded potentials for the triton exit channel. In Sec. IV the spin and parity attributions are discussed while Sec. V contains an outline of our shell-model calculations and the comparison between the experimental and calculated spectrum. Section VI presents a summary of our conclusions.

II. EXPERIMENTAL PROCEDURE

In the present investigation the ^{122}Sn$(p,t)^{120}$Sn experiment has been carried out using the 26 MeV proton beam from the Garching HVEC MP Tandem. The 1.8 m long focal plane detector for light ions [33] performed the particle identification of the ejectiles in the Q3D magnetic spectrograph with an energy resolution of about 8 keV, essentially due to the target thickness. The Sn isotopic enriched target (^{124}Sn 0.55%, ^{122}Sn 96.00%, ^{120}Sn 2.20%, ^{119}Sn 0.30%, ^{118}Sn 0.61%, ^{117}Sn 0.12%, ^{116}Sn 0.22%) had a thickness of 134μg/cm^2 on a carbon backing of 19μg/cm^2.

The cross section angular distributions were measured from 5° to 75° in steps of 5° and from 15° to 25° in steps of 2.5° in two different magnetic field settings in order to reach an excitation energy of the residual nucleus of $\sim$3500 keV. The setting of spectrograph entrance slits provided for $\theta = 5°$ a solid angle of 2.98 msr and for $\theta \geqslant 10°$ a solid angle of 11.04 msr. The beam current intensity was between 300 and 600 nA.

Absolute cross sections were calculated taking into account effective target thickness, solid angle and collected charge, and are estimated with a systematic uncertainty of $\pm 15\%$. Areas and centroids of the triton peaks were determined by means of the computer code AUTOFIT [34], using as reference the shape of the triton peak at 2161 keV.

The high resolving power of the magnetic spectrograph, the reduced background and the energy resolution of the spectra allowed us to resolve and analyze a large number of levels, the weakest of them having cross sections as low as 1μb/sr at the maximum in the angular distributions. For the energy calibration of the spectra a polynomial of rank four was used and the parameters of the polynomial were fixed, in the energy range from 0 up to 3500 keV, imposing the reproduction of the following energies reported on the Kitao *et al.* prepublication of the adopted level scheme of ^{120}Sn [27]: 1875.107, 2194.292, 2284.26, 2355.382, 2400.29, 2420.90, 2465.633, 2587.39, 3057.943, 3179.08, 3386.32, and 3471.54 keV. Our quoted energies are estimated to have an uncertainty of ± 3 keV.

In Fig. 1 the triton spectrum at 10° is shown and the excitation energies of the most prominent peaks are indicated. The position of the ground states for the different Sn isotopes are identified on the basis of *Q*-value differences [35] and the correctness of the attributions was also verified reconstructing the cross sections angular distribution for each of the isotopes [36]. The ground state of ^{122}Sn is outside the range covered by measured magnetic settings. Owing to the chemical purity of the target and the isotopic enrichment,

only the most intense transitions of each contaminant may give an observable yield.

We have studied 38 (p,t) transitions to the final states of ^{120}Sn. Several states not reported on the adopted level scheme [27] have been identified and their spin and parity have been assigned by the DWBA analysis reported in the next section.

The excitation energies of the ^{120}Sn measured in the present experiment with the attributed spin and parity values are given in Table I, together with the energies, spins, and parities of the ^{120}Sn levels adopted so far [27] and with those observed in the previous (p,t) study of Ref. [11]. This table is relevant to the problem of how complete is the spectroscopic information provided by different reactions [37]. Following the arguments of Ponomarev *et al.* [38] in their study on even Nd isotopes, also in the present case, in spite of the (p,t) claimed selectivity, it is possible to study states in ^{120}Sn that are hardly identified in other less selective reactions. In fact, at an excitation energy below 3.5 MeV the number of ^{120}Sn states we have identified and for which the spin and parity values have been unambiguously assigned in the present (p,t) experiment is 29, in comparison with 11 from (p,p') reaction and 20 from $(n,n'\gamma)$ reaction, as reported in Ref. [27]. It is also to be noted that of the 38 studied levels, 7 are seen for the first time.

III. DWBA CALCULATIONS

A DWBA analysis of the experimental reaction data has been carried out in the cluster pick-up model. The calculations have been done in finite range approximation, using the computer code DWUCK5 [39].

In this analysis, both the light-particle form factor (LPFF) and the heavy-particle form factor (HPFF) were calculated using a Woods-Saxon potential. The number of nodes in the radial bound-state wave function is given by the conservation rule for harmonic oscillator quanta

$$Q=2N+L=\sum_{i=1}^{2}(2n_i+l_i), \tag{1}$$

where n_i and l_i are the quantum numbers of the individual nucleons, which form the di-neutron cluster. The two transferred neutrons are supposed to be in a relative $l=0$ state with total spin $S=0$.

As optical potential in the proton channel, a Woods-Saxon potential has been used with parameters deduced by Varner *et al.* [40] in the framework of a global analysis of elastic proton and neutron scattering data. In order to calculate the real part of the triton-nucleus potential, a double-folding procedure has been applied following the model of Kobos *et al.* [41]. Up to now, microscopic potentials for triton elastic scattering had been used by Sanderson *et al.* [42] and Cook [43]. The DWBA analysis of the (p,t) reaction ^{90}Zr$(p,t)^{88}$Zr was also performed using a double-folded triton-nucleus potential [44].

The double-folded potential is described by

$$U_F(\vec{r})=\int d^3\vec{r}_1\int d^3\vec{r}_2\rho_T(\vec{r}_1)\rho_t(\vec{r}_2)v(\vec{s},E,\rho), \tag{2}$$

with $\vec{s}=\vec{r}+\vec{r}_1-\vec{r}_2$ and $\vec{r}$ the separation of the centers of mass between target nucleus and triton. $\rho_T(\vec{r}_1)$ and $\rho_t(\vec{r}_2)$ are the respective nucleon densities resulting from electron scattering experiments [45] and unfolded from the finite-charge distribution of the proton.

For $v(E,\rho,\vec{s})$ an effective nucleon-nucleus interaction (TUE3Y) has been chosen which is derived from the G-matrix calculated in a nuclear matter approach using the Bonn one-boson-exchange potential [46]. The NN-interaction is parametrized in terms of a local density- and energy-dependent two-body interaction. This means that, at variance with the usual approach, we do not factorize the interaction $v(\vec{s},E,\rho)$ in a distance- and a energy-density-dependent part, the latter being adjusted phenomenologically.

Using this folded potential, the optical triton-nucleus potential is given by

$$U_{\rm opt}=\lambda U_F(r)+iW(r)+V_{\rm ls}(r)\vec{l}\cdot\vec{s}+V_{\rm Coul}(r), \tag{3}$$

where λ is an overall normalization factor for the real part of the potential, $W(r)$ is given by a Woods-Saxon, and $V_{\rm ls}$ by a Thomas form factor. The Coulomb potential $V_{\rm Coul}(r)$ is assumed to be due to a uniform charge distribution of radius $R_{\rm Coul}=1.25A^{1/3}$ fm. Using this potential we have performed optical model calculations in order to describe the differential cross sections for elastic scattering of tritons on five tin isotopes at $E_t=20$ MeV [47]. A good agreement is found between the experimental and calculated curves. The potential parameters which have been extracted from the calculations for the five tin isotopes are very similar to each other. As a result we get a normalization factor $\lambda\approx1.05$ and volume integrals for the real and imaginary part $I_R\approx385$ MeV fm^3 and $I_I\approx80$ MeV fm^3, respectively. The depth of the spin-orbit potential is about $V_{\rm ls}\approx5$ MeV.

In a first step of the DWBA analysis the ground-state transition of the (p,t) reaction was fitted with the program TROMF [48], which allows a simultaneous fit to both the reaction data and the elastic scattering data in the entrance and exit channel [49]. As starting values for this fit we used the triton potential extracted in the optical model analysis mentioned above and the proton potentials given by Varner *et al.* [40]. In Fig. 2 experimental data for proton elastic scattering on ^{122}Sn at $E_p=30.4$ MeV [50], triton elastic scattering on ^{120}Sn at $E_t=20$ MeV [47] and our (p,t) data for the g.s. transition are compared with the corresponding calculated results. Both the optical potential and form-factor parameters found in this simultaneous fit are given in Table II. The resulting values of the volume integrals of the real and imaginary part for protons and tritons, are $I_R=416$ MeV fm^3, $I_I=106$ MeV fm^3 and $I_R=401$ MeV fm^3, $I_I=76$ MeV fm^3, respectively.

The optical potential parameters differ only slightly from the starting values of the fit procedure. As can be seen in Fig. 2, a good agreement is found between the experimental and calculated results. In order to get this agreement in the case

TABLE I. In columns 1 and 2 are listed the adopted energies, spins, and parities [27] of the ^{120}Sn levels; in columns 3 and 4 the energies and the transferred angular momentum L reported by Fleming *et al.* [11] in the previous (p,t) measurement; in columns 5 and 6 the energies, spins, and parities observed in the present work; in columns 7 and 8 the relative spectroscopic factors S_r and the integrated cross sections from 5° to 75°. Our quoted energies are estimated to have an uncertainty of ± 3 keV. Absolute cross sections are estimated with a systematic uncertainty of $\pm 15\%$.

^{120}Sn level scheme							
Adopted [27]		(p,t) [11]		Present work			
E_{exc} keV	J^π	E_{exc} keV	L	E_{exc} keV	J^π	S_r	σ_{int} (μb)
0.0	0^+	0	0	0	0^+	1	2505.28
1171.265	2^+	1175	2	1171	2^+	0.60	727.72
1875.107	0^+	1880	0	1874	0^+	0.025	34.97
1930							
2097.201	2^+			2099	2^+	0.002	3.02
2159.930	0^+			2161	0^+	0.013	48.57
2170.3	$(+)$						
2194.292	4^+	2190	4	2195	4^+	0.032	67.78
2230							
2252							
2284.26	5^-			2282	5^-	0.45	292.93
2290	$0^+,1^+$	2300	5				
2317	$0^+,1^+$						
2355.382	2^+			2356	2^+	0.034	118.62
2360	3^-	2365	2				
2400.29	3^-			2400	3^-	0.20	361.06
2420.90	$2(^+)$	2420	3	2421	2^+	0.060	195.09
2440	3^-	2440					
2465.633	(4^+)			2465	4^+	0.082	170.75
2481.61	$(7)^-$			2480	7^-	0.59	114.57
2547	(5^-)						
2587.39	(0^+)			2587	0^+	0.025	87.18
2595							
2630	$0^+,1^+$	2620	0				
2643.350	4^+			2643	4^+	0.008	18.46
2685.15	$(6)^+$						
2687	(8^+)						
				2691	$(2^+ + 6^+)$		36.81
2695.93	4^-						
2728.11	2^+			2728	2^+	0.026	35.16
2749.70	$(6)^-$			2751	4^+	0.002	4.92
2800.04	5^-			2801	5^-	0.048	15.08
2802	$(7^-,8^+)$						
2835.39	1^+						
2836.51	(8^+)						
				2840	$(1^- + 8^+)$		31.91
2844	$1^+,2^+,3^+$						
2844.33	$(6)^-$						
2857.61	(0^+)						
2902.21	(10^+)						
2930.53	2^+			2931	$(2^+,3^-)$	0.019–0.044	30.51
2975.68	4^-			2976	$(4^+,5^-)$	0.003–0.012	3.73
2990							
				3009	2^+	0.0005	1.23
3034.78							
3057.943	4^+	3050		3059	4^+	0.17	170.22

TABLE I. (*Continued*).

^{120}Sn level scheme							
Adopted [27]		(p,t) [11]		Present work			
E_{exc} keV	J^π	E_{exc} keV	L	E_{exc} keV	J^π	S_r	σ_{int} (μb)
3069.74	3,4,5						
3077.38	$3(^+)$						
				3100	(1^-)	0.007	5.94
3120							
3157.97	2^+			3159	2^+	0.012	19.05
3179.08	4^+	3170		3179	4^+	0.31	312.86
3208.54	$1^+,2^+,3^+$			3208	0^+	0.008	15.67
3231.95	1,2,3						
3237.32							
				3252	5^-	0.023	7.28
3262.88							
3279.29							
				3280	(1^-)	0.016	14.60
3284.62	1,2						
3330							
				3341	(3^-+4^+)		12.46
3349.92	$(4)^+$						
3386.32	1,2			3388	$(2^+,3^-)$	0.0078–0.0079	11.12
3438.25	(4)			3442	$(4^+,5^-)$	0.007–0.020	15.05
3446.47	$(7^-,8^-)$						
				3455	(3^-+7^-)		31.57
3471.54	(3^-)			3470	3^-	0.027	18.95

of the (p,t) reaction, the calculated differential cross sections have to be multiplied by an overall normalization factor $N=1.52$.

Using the potential and form factor parameters deduced in this simultaneous fit, we have subsequently calculated the cross sections for all (p,t) transitions to the excited states. The experimental data and the results of the calculations are compared in Figs. 3–5. The relative spectroscopic factors, obtained by fitting the calculated cross sections to the experimental data and normalized to the g.s. transition, are listed in the last but one column of Table I.

Generally a good agreement is found between the experimental and calculated results. In particular, the positions of the first maximum in the angular distributions, which are correlated with the transferred angular momentum L, are well described by the DWBA calculations. For $L=0$ transitions the first maximum is observed in the forward direction. Strong oscillating angular distributions result from the DWBA calculations. Experimentally this behavior is observed only for the g.s. transition. The angular distribution of transitions to excited 0^+ states are more or less smeared out, but the strong increase of the cross section towards forward angles remains as a criterion for a $L=0$ transfer. This effect of smearing-out is well known and can be traced to collective properties of excited 0^+ states in even Sn nuclei [24,51].

IV. SPIN AND PARITY ATTRIBUTIONS

In the present experiment most transitions exhibit angular distributions whose shapes strongly depend on L-transfer values, as mentioned above. Since only natural-parity states are allowed in the one-step (p,t) reaction process, each final level excited by the pick-up of a neutron pair from the even-even target ^{122}Sn ($J^\pi=0^+$) will be populated with a unique L transfer, thus leading to an unambiguous assignment of spin and parity to the final states. As previously done in choosing the reference lines used for the energy calibration, also in the discussion of spin and parity attributions we will refer to the Kitao *et al.* prepublication of the adopted level scheme of ^{120}Sn [27].

For the excited levels up to 2400 keV in ^{120}Sn, our spin and parity assignments, deduced from the comparison of the measured angular distribution and the theoretical predictions, agree with the values reported in the adopted level scheme [27]. A large body of data supports the spin and parity assignments to the g.s. and the first excited states in this energy region. For the levels at 2421 keV ($J^\pi=2^+$), 2465 keV ($J^\pi=4^+$), 2480 keV ($J^\pi=7^-$), 2587 keV ($J^\pi=0^+$), 2643 keV ($J^\pi=4^+$), 2728 keV ($J^\pi=2^+$), 2801 keV ($J^\pi=5^-$), 3059 keV ($J^\pi=4^+$), 3159 keV ($J^\pi=2^+$), 3179 keV ($J^\pi=4^+$), and 3470 keV ($J^\pi=3^-$), we confirm the adopted assignments [27], while we remove the uncertainties when a tentative assignment is made. The proposed assignments for all the other levels observed in this study are discussed.

2691 keV level. In the adopted level scheme [27] there are two close lying levels, the first at 2687 keV with tentative (8^+) assignment derived from a (p,p') study [1], and the second at 2695.93 keV with 4^- assignment from a $(n,n'\gamma)$

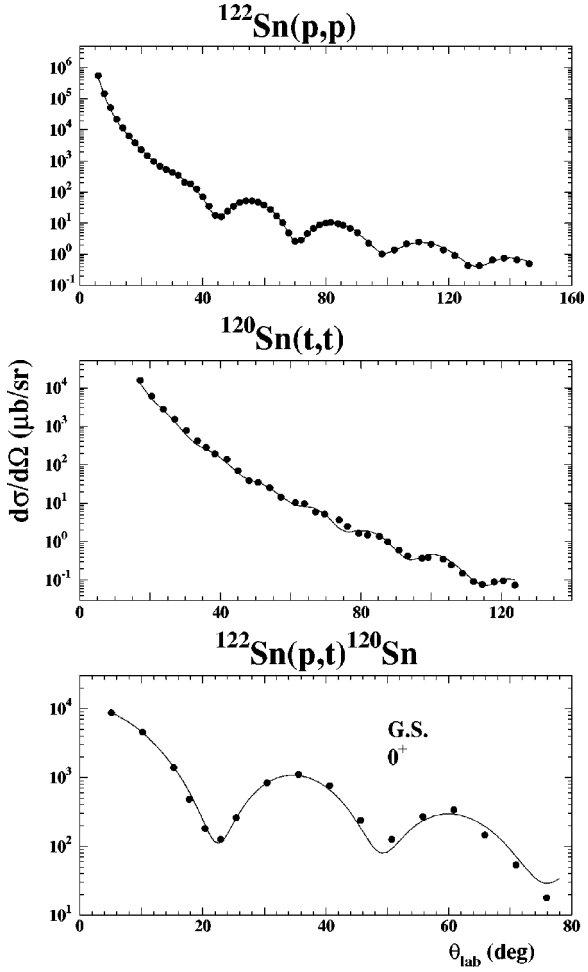

FIG. 2. The experimental data for proton elastic scattering on ^{122}Sn [50], for triton elastic scattering on ^{120}Sn [47], and the experimental (p,t) data for the ^{120}Sn g.s. transition are compared with the calculations.

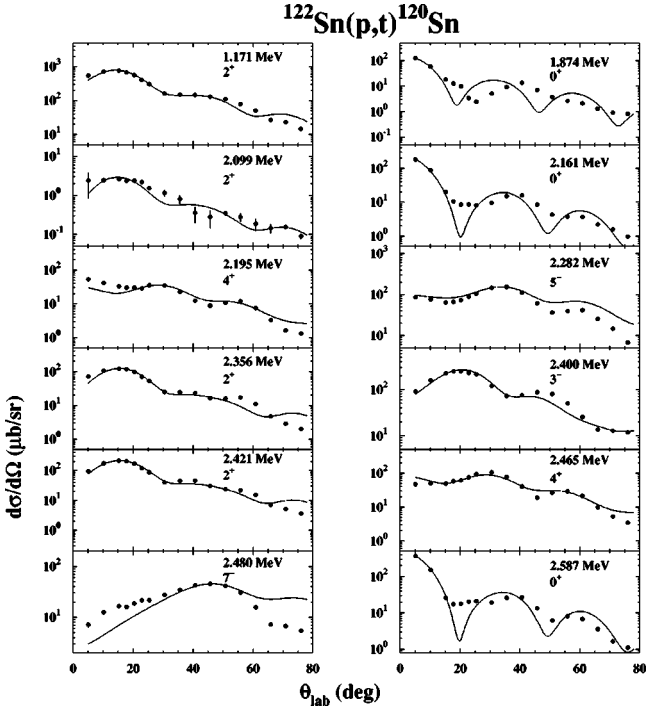

FIG. 3. Angular distributions for the transitions to the ^{120}Sn levels whose excitation energy, spin, and parity are indicated. The dots represent the experimental data, the solid lines the theoretical estimates obtained with the double-folded triton potential. The energies attributed to the observed levels are those given in the present work.

study [23]. Furthermore, a level at 2685.20 keV is reported on the basis of a $(n,n'\gamma)$ study [23] with a $(6)^+$ assignment. We obtain a good reproduction of the angular distribution by considering an unresolved doublet with $J^\pi=2^+$ (10%) and $J^\pi=6^+$ (90%).

2751 keV level. In Ref. [27] a level at 2749.70 keV is given on the basis of a $(n,n'\gamma)$ study [23] with a $(6)^-$ assignment. In our measurement the level at 2751 keV is quite weakly populated and the angular distribution is reproduced by a $L=4$ transfer. The present attribution is $J^\pi=4^+$.

2840 keV level. In the adopted level scheme [27] there are two close lying levels observed in a $(n,n'\gamma)$ study [23], the first at $E=2835.39$ keV with a spin and parity 1^+, and the second at 2836.51 keV with a tentative spin and parity (8^+). Furthermore a level at 2844 keV is reported with a tentative spin and parity assignment $1^+,2^+,3^+$ deduced from a ^{119}Sn(d,p) reaction study [7]. In our measurement this group of levels is weakly populated and the angular distribution is quite well reproduced by considering an unresolved doublet with $J^\pi=1^-$ (3%) and $J^\pi=8^+$ (97%).

2931 keV level. In the adopted level scheme [27] a level is reported at $E=2930.53$ keV obtained from (d,p) [7], (p,p') [1] and $(n,n'\gamma)$ [23] studies with $J^\pi=2^+$. In our (p,t) mea-

TABLE II. The Woods-Saxon optical model parameters for the incident proton, the value of the normalization factor λ, the parameters of the imaginary Woods-Saxon triton-nucleus potential used with the double-folded real potential, and the geometrical parameters of the form factors.

	Optical model parameter													
	V_r (MeV)	r_r (fm)	a_r (fm)	λ	W_v (MeV)	r_v (fm)	a_v (fm)	W_d (MeV)	r_d (fm)	a_d (fm)	V_{ls} (MeV)	r_{ls} (fm)	a_{ls} (fm)	r_c (fm)
p	50.2	1.21	0.69		1.9	1.25	0.69	8.0	1.21	0.69	5.9	1.10	0.63	1.26
t				1.10	14.3	1.50	0.83				4.7	1.42	0.39	1.25
HPFF (WS)		1.28	0.58											
LPFF (WS)		1.30	0.50											

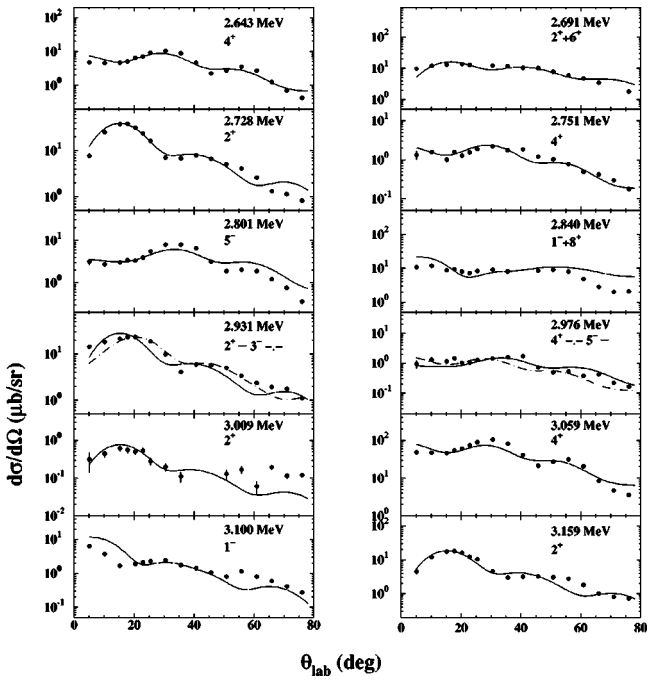

FIG. 4. Same as Fig. 3.

surement the level at 2931 keV is quite populated and the angular distribution can be reproduced by both $L=2$ and $L=3$. The present tentative assignment is $J^{\pi}=(2^{+},3^{-})$.

2976 keV level. In the adopted level scheme [27] a level is reported at $E=2975.68$ keV obtained from a (p,p') [1] and $(n,n'\gamma)$ studies [23] with spin and parity 4^{-}. In our (p,t) measurement the level at 2976 keV is populated quite weakly and the angular distribution is reasonably reproduced by $L=5$ or also by $L=4$. The present tentative assignment is $J^{\pi}=(4^{+},5^{-})$

3009 keV level. At this energy no level is given in the adopted level scheme [27]. In our case this level is populated very weakly. We reproduce fairly well the measured angular distribution with an $L=2$ transfer. The present assignment is $J^{\pi}=2^{+}$.

3100 keV level. At this energy no level is given in the adopted level scheme [27]. A state at 3090 ± 20 keV is reported by Leonard [9] from unpublished results of a ^{121}Sb$(d,{}^{3}$He) study. In that study an $L=1$ transfer is assumed. In our measurement this level is reasonably populated and the angular distribution is compatible with a tentative attribution of $J^{\pi}=(1^{-})$.

3208 keV level. In Ref. [27] a level is given with an energy 3208.54 keV with a spin and parity assignment of 1^{+}, 2^{+}, and 3^{+} resulting from an $L=2$ transfer in a ^{119}Sn$(d,p)^{120}$Sn reaction study [7]. From the ^{120}Sn$(n,n'\gamma)$ reaction [23] a level is reported at this energy with tentative spin and parity attribution of (0^{+}). In our case the 3208 keV level is quite strongly populated and the angular distribution is reasonably well reproduced by a $L=0$ transfer. The present assignment is $J^{\pi}=0^{+}$.

3252 keV level. At this energy no level is given in the adopted level scheme [27]. This level is weakly populated in our experiment. The measured angular distribution is consistent with an attribution of 5^{-}.

3280 keV level. In Ref. [27] a level is given at an energy of 3279.29 keV derived from a $(n,n'\gamma)$ [23] study. In Ref. [23] the spin attribution is 1. In our experiment we find a weakly populated level. We reproduce the angular distribution by assuming an $L=1$ transfer. The present tentative assignment is $J^{\pi}=(1^{-})$.

3341 keV level. In Ref. [27] two levels are reported, one with $E=3330\pm10$ keV derived from a (p,p') study [1] without spin and parity attribution and another one at 3349.92 keV which was observed in a ^{120}In β decay [17,18], and in the $(n,n'\gamma)$ reaction [23] with $(4)^{+}$ spin and parity attribution. In our study this level is strongly populated. We reproduce the angular distribution quite well by considering an unresolved doublet with $J^{\pi}=3^{-}$ (40%) and $J^{\pi}=4^{+}$ (60%).

3388 keV level. In the adopted level scheme [27] a level is denoted with an energy of 3386.32 keV on the basis of the (p,p') [1], (d,p) [7], and $(n,n'\gamma)$ [23] studies with 1, 2 spin attribution. In our measurement this level is quite strongly populated. The angular distribution is well reproduced by both $L=2$ and $L=3$ transfer. The present tentative assignment is $J^{\pi}=(2^{+},3^{-})$.

3442 keV level. In the adopted level scheme [27] a level is given at 3438.25 keV identified in ^{120}In β decay (46.2 s) studies [17,18] and in $(n,n'\gamma)$ reaction [23] with a (4) spin attribution. In our case the level is strongly populated. The angular shape is reproduced by both $L=5$ and $L=4$ transfer. The present tentative assignment is $J^{\pi}=(4^{+},5^{-})$.

3455 keV level. In Ref. [27] a level is reported at $E=3446.47$ keV from ^{120}In β-decay studies (47.3 s) [17,18] with attributed spin and parity $(7^{-},8^{-})$. We observe a strongly populated level and reproduce quite well the differential cross section by considering an unresolved doublet with $J^{\pi}=3^{-}$ (10%) and $J^{\pi}=7^{-}$ (90%).

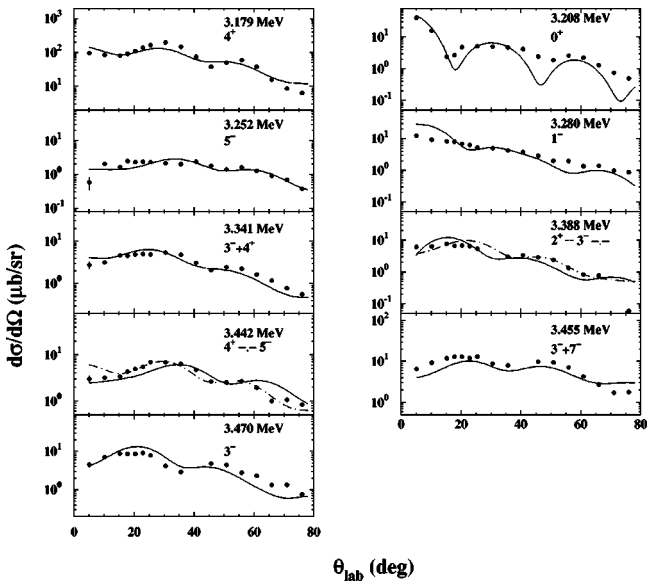

FIG. 5. Same as Fig. 3.

V. SHELL-MODEL CALCULATIONS AND COMPARISON WITH EXPERIMENT

A. Outline of the CCM and calculations

The general shell-model Hamiltonian for a system of identical particles is written as

$$H=\sum_j \epsilon_j \hat{N}_j + \frac{1}{4}\sum_{j_1 j_2 j_3 j_4 JM} G_J(j_1 j_2 j_3 j_4) A^\dagger_{JM}(j_1 j_2) A_{JM}(j_3 j_4), \tag{4}$$

where the ϵ's are the sp energies and $\hat{N}_j$ is the number operator for level j,

$$\hat{N}_j=\sum_m a^\dagger_{jm} a_{jm}. \tag{5}$$

The operator

$$A^\dagger_{JM}(j_1 j_2)=\sum_{m_1 m_2}\langle j_1 m_1 j_2 m_2|JM\rangle a^\dagger_{j_1 m_1} a^\dagger_{j_2 m_2} \tag{6}$$

creates a pair of particles coupled to angular momentum (JM), and the quantities $G_{JM}(j_1 j_2 j_3 j_4)$ are the matrix elements of the two-body interaction between states which are antisymmetrized but not normalized.

The main feature of the CCM is to solve the Schrödinger equation for a nucleus with N valence particles

$$H|N,\beta,J,M\rangle=E_{\beta J}(N)|N,\beta,J,M\rangle, \tag{7}$$

expanding the wave functions in terms of states of the $(N-2)$-particle system. Therefore, we write

$$|N,\beta,J,M\rangle=\sum_{j\gamma} c^J_{j\beta\gamma}(N) A^\dagger_{00}(jj)|N-2,\gamma,J,M\rangle, \tag{8}$$

where β and γ specify the states with N and $N-2$ particles, respectively.

As already mentioned in the Introduction, this implies solving the N-particle problem through a chain calculation involving only nuclei differing by two in nucleon number. In other words, the solution for the N-particle problem is built by starting from an initial value of N, say N_0, and then progressively adding pairs of particles up to the desired value of N. Since only zero-coupled operators are included in the expansion (8), the maximum seniority $v_{\max}$ in the states with N particles is that of the core states $|N-2,\gamma,J,M\rangle$. It is therefore clear that the initial value N_0, at which one starts the chain calculation, determines the seniority truncation, namely $v_{\max}=N_0$ for any value of $N>N_0$.

The practical value of this approach lies in the fact that, within a given seniority truncation, a variety of approximations can be produced by restricting the number of core states in Eq. (8). We call kth order theory the approximation in which the core states are restricted to the lowest k states. This allows for the reduction of the amount of numerical work required by a standard seniority-truncated shell-model calculation.

Our calculations for ^{120}Sn have been carried out within the framework of the CCM including states with seniority v up to 4. We have verified that the use of a 50th-order calculation suffices to produce practically exact results for at least the ten lowest states for each value of the angular momentum. In this way, the size of the matrices to be diagonalized is largely reduced. As an example, within the chosen model space the total number of basis states with $J^\pi=4^+$ is 5409 while our energy matrix is of order 250.

We may mention that inherent in our formalism is the use of the overcomplete set of basis vectors $A^\dagger_{00}(jj)|N-2,\gamma,J,M\rangle$. An account of our procedure for removing the redundant states may be found in Refs. [29] and [52].

As residual interaction between the valence neutrons outside doubly magic ^{100}Sn, we have used a two-particle effective interaction derived from the Paris nucleon-nucleon potential. A description of how this derivation is carried out is given in Ref. [53], where a list of relevant references can also be found. Here, we only emphasize that no adjustable parameter appears in the calculation of our two-body matrix elements.

As regards the sp energies, we have derived them directly from the experimental spectrum of ^{131}Sn. The five levels observed in this nucleus below 2.5 MeV excitation energy are, according to the conclusions of Refs. [54,55], single-neutron hole states. Their corresponding energies are (in MeV): $\epsilon^{-1}_{d_{3/2}}=0.0$, $\epsilon^{-1}_{h_{11/2}}=0.242$, $\epsilon^{-1}_{s_{1/2}}=0.332$, $\epsilon^{-1}_{d_{5/2}}=1.655$, and $\epsilon^{-1}_{g_{7/2}}=2.434$. The sp energies can be obtained [56] from these values through

$$\epsilon_j=-(\epsilon_j^{-1}+\Delta_j), \tag{9}$$

where

$$\Delta_j=\frac{1}{2j+1}\sum_{j'J}(2J+1)G_J(jj'jj'). \tag{10}$$

In this way, we obtain for the sp spectrum the values (in MeV): $\epsilon_{g_{7/2}}=0.0$, $\epsilon_{d_{5/2}}=0.591$, $\epsilon_{d_{3/2}}=2.382$, $\epsilon_{s_{1/2}}=2.141$, and $\epsilon_{h_{11/2}}=2.988$.

Clearly, the above choice may not be the best one, as significant changes in the nuclear mean field are to be expected when moving away from closed shells. In this study, however, we did not want to play with adjustable parameters.

B. Comparison between theory and experiment

In Fig. 6 the spectrum of ^{120}Sn established in the present experiment is compared with the calculated one. In the theoretical spectrum we include all the levels up to 3.0 MeV while in the higher-energy region only states having the same angular momenta and parities as those of the observed ones are reported.

As a general remark, let us note that in the energy interval 2.7–3.2 MeV the theoretical level density is smaller than the observed one (see Fig. 6). This may be attributed to the lack

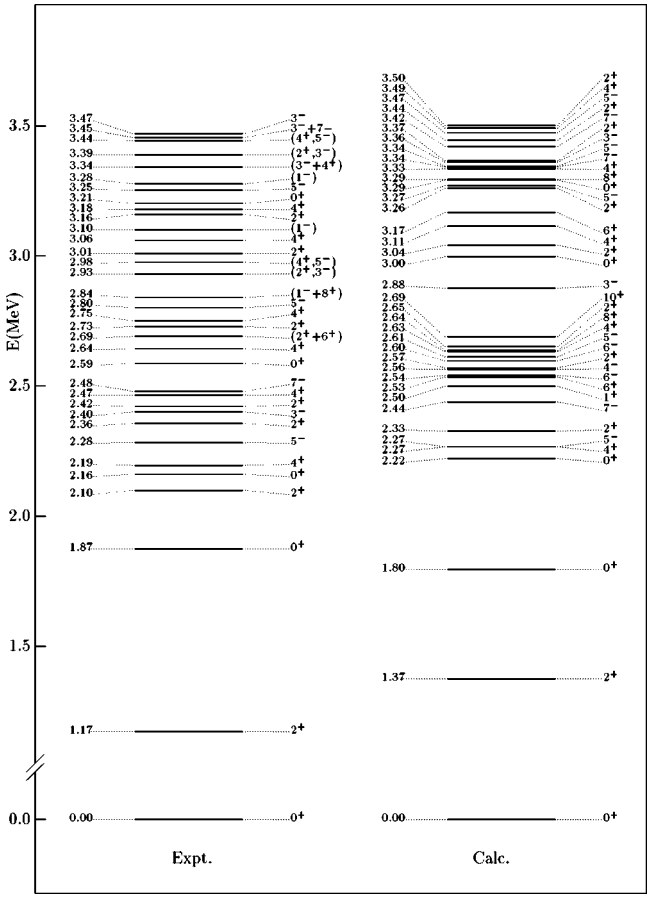

FIG. 6. Comparison of experimental and shell model spectra. See text for comments.

of configurations with $v>4$, which are likely to produce a downshift of most of the high-lying states. This is indicated by the fact that, except the 1^+ state, all the states up to about 2.7 MeV have dominant $v=0$ or 2 components while above this energy there is in general a strong seniority mixing. Thus, rather large discrepancies are to be expected in the higher-energy region.

We now compare in some detail the calculated and experimental spectra. From Fig. 6 we see that the experimental low-energy spectrum is well reproduced by the theory. In fact, up to 2.3 MeV a one-to-one correspondence between the six lowest calculated and experimental levels can be unambiguously established. As regards the quantitative agreement, a rather large discrepancy (about 200 keV) occurs only for the two 2^+ states, the calculated excitation energies of the other four states differing by less than 80 keV from the experimental ones.

Four of the next five excited levels in the observed spectrum, namely, those with $J^\pi=2^+$ (twice), 4^+, and 7^-, can be identified with calculated states located in the energy interval 2.4–2.7 MeV, the agreement between theory and experiment being comparable with that obtained for the lower-energy region. Our results, therefore, confirm the spin-parity assignments made in the present work for the states at 2.42, 2.47, and 2.48 MeV, which had not received until now a firm assignment [27]. Concerning the 3_1^- state at 2.40 MeV, the calculated energy is considerably higher (about 500 keV) than the experimental one. This is not surprising since configurations outside of our model space are likely to be important for this state. Besides the four above states, other eight states are predicted by the theory in the energy range 2.4–2.7 MeV. For three of them an identification with observed levels may be attempted. In particular, the 5^- state can be associated to the 5^- level at 2.80 MeV, while the 6^+ and 8^+ states can each be identified with the higher spin member of the $J^\pi=2^++6^+$ and $J^\pi=1^-+8^+$ unresolved doublets at 2.69 and 2.84 MeV, respectively. Regarding the 2^+ member of the first doublet, no correspondence with a given calculated level can be safely established, as it appears from Fig. 6. As for the 1^- member of the second doublet, our first calculated state with this angular momentum and parity is predicted at 3.9 MeV. It therefore appears that this state, as well as the two other experimental 1^- states at 3.10 and 3.28 MeV, respectively, are beyond the scope of the present calculation. It is of interest to note that a 10^+ state is predicted by the theory 50 keV above the 8^+ one. This state can be identified with the experimental 10^+ isomer, deexciting to the 8^+ state (2.84 MeV) by the 68.7 keV $E2$ transition [57]. It should also be noted that four states with $J^\pi=1^+$, 4^-, and 6^- (twice) are predicted at 2.50, 2.56, 2.54, and 2.60 MeV, respectively. However, as already mentioned in Sec. IV, these unnatural parity states are not excited in a one-step (p,t) reaction.

The identification of any of the other experimental levels above 2.5 MeV with states predicted by the theory may be misleading. For example, the calculated 0^+ and 4^+ states at 3.00 and 3.11 MeV might be identified with the experimental 0^+ and 4^+ levels at 2.59 and 2.64 MeV, respectively, with discrepancies of about 400–500 keV. In this context, it should be considered that these two states are characterized by a strong seniority mixing, which is likely to make our $v \leqslant 4$ truncation too restrictive. As mentioned above, this argument may also hold for most of the states in this energy region. It is worth noting, however, that in the theoretical spectrum we have, for any given J^π (except the 1^- states discussed above), all the states which appear in the experimental one (this is not quite evident from Fig. 6, where the calculated states are reported only up 3.5 MeV).

VI. SUMMARY

In a high resolution experiment cross section angular distributions have been measured for transitions to 38 levels of the ^{120}Sn nucleus, up to an excitation energy of $\sim$ 3.5 MeV in the (p,t) reaction induced on ^{122}Sn at 26 MeV proton incident energy. The experimental reaction data have been analyzed using a double-folding procedure to calculate the real part of the triton-nucleus potential in the framework of the model of Kobos *et al.* [41]. The effective nucleon-nucleon interaction is calculated in a nuclear matter approach from the Bonn one-boson-exchange potential and is parametrized in term of a local density- and energy-dependent two-body interaction. The DWBA calculations have been performed in the finite-range approximation, with a cluster form factor.

Exploiting the remarkable dependence of the transferred angular momentum displayed by the differential angular distributions, we have improved the knowledge of the ^{120}Sn level scheme. In fact, we have removed the uncertainty in spin-parity assignment for five levels and given an unambiguous assignment, which is different from that of Ref. [27], to two states. Furthermore, we have assigned spin and parity to two new levels.

In connection with the experimental work, we have carried out a theoretical study of ^{120}Sn within the framework of the shell model. We have truncated the model space to states with $v \leqslant 4$ and made use of a two-body effective interaction derived from the nucleon-nucleon Paris potential. The comparison of the calculated spectrum with the experimental one lends support to some of the spin-parity assignments given in this work. However, above about 2.7 MeV excitation energy, a one-to-one correspondence between calculated and observed levels could not be established. This is because in this energy region our calculations are likely to be not accurate enough to reproduce the details of the spectrum. In fact, while collective components may play an important role in the structure of some states, our seniority truncation is certainly too restrictive. We would also like to point out that we have not tried to optimize the sp energies. In fact, within the framework of the shell model, changes in the sp energies are to be expected when going several nucleons far from the closed shell.

ACKNOWLEDGMENTS

We thank J. Weil for valuable comments. One of us (M.J.) wishes to express his gratitude to the Sektion Physik of the LMU for hospitality and acknowledges the financial support of the Istituto Nazionale di Fisica Nucleare. This work was supported in part by grants of the Beschleunigerlaboratorium, the DFG under Grant No. C4-Gr894/2, and the Italian MURST.

[1] O. Beer, A. El Behay, P. Lopato, Y. Terrien, G. Vallois, and K. K. Seth, Nucl. Phys. **A147**, 326 (1970); D. A. Allan, B. H. Armitage, and B. A. Doran, Nucl. Phys. **66**, 481 (1965).
[2] R. K. Jolly, Phys. Rev. **139**, B318 (1965).
[3] T. Yamagata, S. Kishimoto, K. Yuasada, K. Iwamoto, B. Saeki, M. Tanaka, T. Fukuda, I. Miura, M. Inoue, and H. Ogata, Phys. Rev. C **23**, 937 (1981).
[4] G. Bruge, J. C. Faivre, H. Faraggi, and A. Bussiere, Nucl. Phys. **A146**, 597 (1970).
[5] V. I. Chuev, Yu. A. Glukhov, V. I. Manko, B. G. Novatskü, A. A. Oglobin, S. B. Sakuta, and D. N. Stepanov, Phys. Lett. **42B**, 63 (1972).
[6] A. Weller, P. Egelhof, R. Caplar, O. Karban, D. Krümer, K. H. Möbius, Z. Moroz, K. Rusek, E. Steffens, G. Tungate, K. Blatt, I. Koonig, and D. Fick, Phys. Rev. Lett. **55**, 480 (1985).
[7] L. R. Norris and C. F. Moore, Phys. Rev. **136**, B40 (1964); E. J. Schneid, A. Prakash, and B. L. Cohen, Phys. Rev. **156**, 1316 (1967).
[8] R. Chapman, M. Hyland, J. L. Durell, J. N. Mo, M. Macphal, H. Sharma, and N. H. Merrill, Nucl. Phys. **A316**, 40 (1979).
[9] R. F. Leonard, Report No. N72-18705, 1972; or NASA TM X-68004.
[10] Z. Basrak, N. Cindro, and M. Turk, Nucl. Phys. **A299**, 381 (1978).
[11] D. G. Fleming, M. Blann, H. W. Fulbright, and J. A. Robbins, Nucl. Phys. **A157**, 1 (1970).
[12] J. H. Bjerregaard, O. Hansen, O. Nathan, L. Vistisen, R. Chapman, and S. Hinds, Nucl. Phys. **A110**, 1 (1968).
[13] E. Gadioli, E. Gadioli Erba, R. Gaggini, P. Guazzoni, P. Michelato, A. Moroni, and L. Zetta, Z. Phys. A **310**, 43 (1983).
[14] J. Jänecke, F. D. Becchetti, and C. E. Thorn, Nucl. Phys. **A325**, 337 (1979).
[15] E. Liukkonen and J. Hattula, Z. Phys. **241**, 150 (1971).
[16] O. Scheidemann and E. Hagebo, J. Inorg. Nucl. Chem. **35**, 3055 (1973).
[17] H. C. Cheung, H. Huang, B. N. Subba Rao, L. Lessard, and J. K. P. Lee, J. Phys. G **4**, 1501 (1978).
[18] S. Raman, T. A. Walkiewicz, L. G. Multhauf, K. G. Tirsell, G. Bonsignori, and K. Allart, Phys. Rev. C **37**, 1203 (1988).
[19] R. J. Pan, D. W. Hatherington, D. B. McConnell, and H. W. Taylor, Can. J. Phys. **48**, 1687 (1970).
[20] M. Campbell, K. W. D. Ledingham, A. D. Baillie, M. L. Fitzpatrick, J. Y. Gourlay, and J. G. Lynch, Nucl. Phys. **A249**, 349 (1975).
[21] S. Kikuchi and Y. Sugiyama, Nucl. Phys. **A223**, 1 (1974).
[22] Y. Schleringer, H. Szichman, G. Ben-David, and M. Mass, Phys. Rev. C **2**, 2001 (1970).
[23] A. M. Demidov and I. V. Mikhailov, Yad. Fiz. **55**, 865 (1992).
[24] N. G. Jonsson, A. Backlin, J. Kantele, R. Julin, M. Luontama, and A. Passoja, Nucl. Phys. **A371**, 333 (1981).
[25] P. H. Stelson, F. K. McGowan, R. L. Robinson, and W. T. Milner, Phys. Rev. C **2**, 2015 (1970).
[26] A. Hashizume, Y. Tendow, and M. Ohshima, Nucl. Data Sheets **52**, 641 (1987).
[27] K. Kitao *et al.*, Prepublication of the adopted level scheme of ^{120}Sn. Information extracted from the ENSDF data base revision of 28-Jan-1999, using the NNDC Online Data Service.
[28] A. Covello, F. Andreozzi, L. Coraggio, A. Gargano, and A. Porrino, in *Contemporary Nuclear Shell Models*, Vol. 482 of *Lecture Notes in Physics* (Springer-Verlag, Berlin, 1997).
[29] F. Andreozzi, L. Coraggio, A. Covello, A. Gargano, and A. Porrino (unpublished).
[30] R. J. Liotta and C. Pomar, Nucl. Phys. **A382**, 1 (1982), and references therein.
[31] M. Lacombe, B. Loiseau, J. M. Richard, R. Vinh Mau, J. Côté, P. Pires, and R. de Tourreil, Phys. Rev. C **21**, 861 (1980).
[32] A. Covello, F. Andreozzi, L. Coraggio, A. Gargano, and A. Porrino, in *New Perspectives in Nuclear Structure*, Proceedings of the Fifth International Spring Seminar on Nuclear Physics, Ravello, 1995, edited by A. Covello (World Scientific, Singapore, 1996), p. 147.

[33] E. Zanotti, M. Bisenberger, R. Hertenberger, H. Kader, and G. Graw, Nucl. Instrum. Methods Phys. Res. A **310**, 706 (1991).
[34] J. R. Comfort, ANL Physics Division, Report No. PHY 19708, Argonne.
[35] A. H. Wapstra and K. Bos, At. Data Nucl. Data Tables **19**, 17 (1977).
[36] G. Cata-Danil, P. Guazzoni, M. Jaskola, L. Zetta, G. Graw, R. Hertenberger, D. Hofer, P. Schiemenz, B. Valnion, E. Zanotti-Müller, U. Atzrott, F. Hoyler, F. Nuoffer, and G. Staudt, J. Phys. G **22**, 107 (1996).
[37] J. Kern, Phys. Lett. B **320**, 7 (1994).
[38] V. Yu. Ponomarev, M. Pignanelli, N. Blasi, A. Bontempi, J. A. Bordewijk, R. De Leo, G. Graw, M. N. Harakeh, D. Hofer, M. A. Hofstee, S. Micheletti, R. Perrino, and S. Y. van der Werf, Nucl. Phys. **A601**, 1 (1996).
[39] P. D. Kunz, computer code DWUCK 5, University of Colorado (unpublished).
[40] R. L. Varner, W. J. Thompson, T. L. McAbee, E. L. Ludwig, and T. B. Clegg, Phys. Rep. **201**, 57 (1991).
[41] A. M. Kobos, B. A. Brown, R. Lindsay, and G. R. Satchler, Nucl. Phys. **A425**, 205 (1984).
[42] D. P. Sanderson, J. A. Carr, and K. W. Kemper, Phys. Rev. C **32**, 1169 (1985).
[43] J. Cook, Nucl. Phys. **A473**, 458 (1987).
[44] M. Jaskola, P. Guazzoni, L. Zetta, J. N. Gu, A. Vitturi, G. Graw, R. Hertenberger, B. Valnion, F. Nuoffer, and G. Staudt, Acta Phys. Pol. B **29**, 385 (1998).
[45] H. de Vries, C. W. de Jeger, and C. de Vries, At. Data Nucl. Data Tables **36**, 495 (1987).
[46] G. Bartnitzky, H. Clement, P. Czerski, H. Müther, F. Nuoffer, and J. Siegler, Phys. Lett. B **386**, 7 (1996).
[47] E. R. Flynn, D. D. Armstrong, J. G. Beery, and A. G. Blair, Phys. Rev. **182**, 1113 (1969).
[48] M. Walz, computer code TROMF, University of Tübingen (unpublished).
[49] M. Walz, R. Neu, G. Staudt, H. Oberhummer, and H. Cech, J. Phys. G **14**, L91 (1988).
[50] A. G. Hardacre, J. F. Turner, J. C. Kerri, G. A. Gard, P. E. Cavanagh, and C. F. Coleman, Nucl. Phys. **A173**, 346 (1971).
[51] A. Bäcklin, N. G. Jonsson, R. Julin, J. Kantele, M. Luontama, A. Passoja, and T. Poikolainen, Nucl. Phys. **A351**, 490 (1981).
[52] F. Andreozzi, A. Covello, A. Gargano, and A. Porrino, in *Proceedings of the International Symposium on Nuclear Shell Models*, Philadelphia, 1984, edited by M. Vallieres and B. H. Wildenthal (World Scientific, Singapore, 1985), p. 610.
[53] F. Andreozzi, L. Coraggio, A. Covello, A. Gargano, T. T. S. Kuo, Z. B. Li, and A. Porrino, Phys. Rev. C **54**, 1636 (1996).
[54] B. Fogelberg and J. Blomqvist, Phys. Lett. **137B**, 20 (1984).
[55] B. Fogelberg and J. Blomqvist, Nucl. Phys. **A429**, 205 (1984).
[56] R. D. Lawson, *Theory of Nuclear Shell Model* (Clarendon Press, Oxford, 1980), Chap. 3.
[57] S. Lunardi, P. J. Daly, F. Soramel, C. Signorini, B. Fornal, G. Fortuna, A. M. Stefanini, R. Broda, W. Meczynski, and J. Blomqvist, Z. Phys. A **328**, 487 (1987).